Natural controls validation for handling elevated fluoride concentrations in extraction activated Tóthian groundwater flow systems: San Luis Potosí, Mexico

Antonio Cardona[1], Andre Banning[2*], José Joel Carrillo-Rivera[3], Alfredo Aguillón-Robles[4], Thomas R. Rüde[5] and Jorge Aceves de Alba[1]

[1] Earth Sciences, Universidad Autónoma de San Luis Potosí, Dr. Manuel Nava No. 8, San Luis Potosí, 78290, Mexico

[2] Hydrogeology Department, Ruhr-Universität Bochum, Universitätsstr. 150, 44801 Bochum, Germany

email: andre.banning@rub.de, tel.: +492343223298

*corresponding author

[3] Institute of Geography, Universidad Nacional Autónoma de México, C.U., Coyoacán, 04510, Mexico City, Mexico

[4] Institute of Geology, Universidad Autónoma de San Luis Potosí, Dr. Manuel Nava No. 5, San Luis Potosí, 78240, México

[5] Institute of Hydrogeology, RWTH Aachen University, Lochnerstr. 4-20, 52064 Aachen, Germany

Abstract: Fluoride concentration in groundwater supply above the guideline value of 1.5 mg/L is a health hazard for the population living in two thirds of the Mexican territory. Enhanced groundwater extraction in the city of San Luis Potosí (SLP), Mexico, led to a substantial territorial increase in water with high fluoride (F^-) which originates from thermal water-rock interaction with regional rhyolites. Previous knowledge of the Tóthian

groundwater flow systems around SLP City and their F^- concentrations from 1987 data provided an insight into natural F^- controls for the construction and operation of boreholes. During the period 1987-2007, the number of new boreholes increased as well as the re-location of boreholes whose production diminished. Overall estimated extraction augmented from 2.6 to 4.1 m^3/s. Results obtained for 2007 suggest that F^- controls defined for 1987 data (e.g. variable portions of F^--rich deep thermal water in borehole yields) are also valid in newly constructed boreholes. Water authority actions related to groundwater extraction lack consideration of proposed F^- controls, so constructed boreholes progressively tapping the high F^- groundwater flow system resulted in a 85 % increase of the F^- affected territory (>2 mg/L) between 1987 and 2007. Reduction in F^- extraction following the proposed natural control mechanisms (e.g. fluorite precipitation) was also confirmed. Applying geochemical and mineralogical analysis, rhyolites surrounding the SLP graben basin and contributing to its volcano-clastic sedimentary filling were identified as the primary F^- source for elevated concentrations in groundwater of the area under investigation.

Keywords: hydrochemistry, fluorosis, arid regions, volcanic aquifer, groundwater management, Mexico

1 Introduction

1.1 Importance of fluoride management

Groundwater is the major source of potable water supply in arid and semi-arid regions. However, its availability may be threatened not only by the introduction of contaminants through human activities but also by natural processes (McArthur et al. 2012; Nicolli et al. 2012; Jia et al. 2014; Edmunds et al. 2015; Banning and Rüde 2015). The contribution of

some minor and trace elements (e.g., fluoride, iron, arsenic, uranium, lead, and cadmium) that change the quality of extracted groundwater is a substantial health hazard in many groundwater regions worldwide (e.g., Edmunds and Smedley 1996; Fendorf et al. 2010; Guo et al. 2014; Jia et al. 2014; Jia et al. 2017; Bjørklund et al. 2017). Recently, the impact of trace elements in the water supply of Mexico has started to be given consideration in groundwater management. Carrillo-Rivera et al. (2002) proposed feasible natural F^- management controls at borehole site without the need of a water treatment plant. These management approaches might be applied elsewhere as F^- is a common natural constituent that threatens groundwater supply in both industrialized and developing countries (e.g., Lucas 1988; Gaciri and Davies 1993; Valenzuela-Vásquez et al. 2006; Amini et al. 2008; Nicolli et al. 2012; Guo et al. 2012; Navarro et al. 2017; Raju 2017). In the semi-arid eastern part of the Sierra Madre Occidental alone, at least some 15 % of the total Mexican population (estimated to be in excess of 110 million people), are supplied with regional F^--rich groundwater.

1.2 Study area

The investigation area is located around San Luis Potosí (SLP) City, capital of the homonymous state, in the semi-arid north-central part of Mexico (Fig. 1). It hosts one of the conurbations of the country with the highest population growing rate (broadly 5-7 % p.a.), and presently has around one million inhabitants.

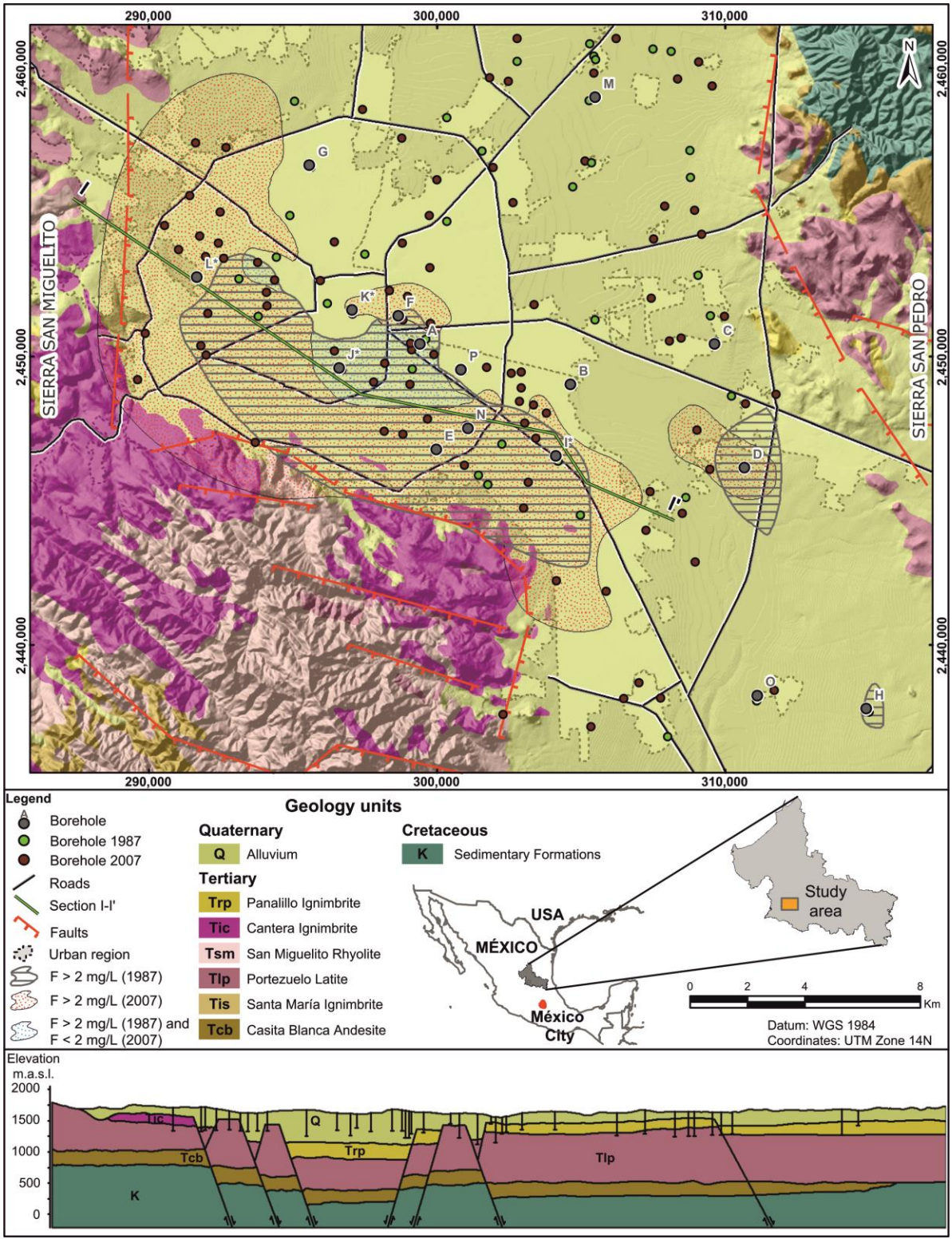

Fig. 1: Morphologic-geological map of the study area (including territories with high groundwater F^- concentrations 1987 and 2007, and location of the sampled boreholes in the SLP graben basin), location of the study area in Mexico, and geological cross section I-I´ (bottom; including the location of sampled boreholes along it). Sources: simplified geological and structural map modified after Labarthe-Hernández et al. (1982) and Tristán-González (1986); digital elevation model from INEGI (2013).

The study area is part of one of the several closed basins existing in the north-central part of Mexico. The steep surrounding mountain ranges of Sierra de San Miguelito (SSM, west of SLP) and Sierra de San Pedro (SSP, east of SLP) consist of Tertiary felsic volcanic and Cretaceous calcareous rocks, respectively (Fig. 1). These sierras have an elevation exceeding 2,300 m a.m.s.l. and slope towards the plane of the drainage basin which has an altitude of about 1,900 m a.m.s.l. The mean annual air temperature is around 17.5 °C, while the summer mean temperature is around 21 °C.

The San Luis Potosí Volcanic Field (SLPVF) is located between the morphotectonic province of Sierra Madre Oriental, and the volcanic province of Sierra Madre Occidental (Guzmán and DeCserna 1963), in the southern part of the Mesa Central. The main local geological features are associated with a thick (>1500 m) sequence of extrusive Tertiary volcanic rocks and alluvial materials, covering a Cretaceous limestone and calcareous mudstone sequence outcropping in folded NW-SE-striking structures in SSP (Fig. 1, cross section); suchlike features are typical for a number of similar basins in the Sierra Madre Occidental (400 km wide and 1,500 km long, hosting volcanic rocks with a total thickness of 2-3 km) and other regions of northwestern Mexico and the southwestern U.S.A. The Tertiary volcanic units relevant for this study were generated in several stages and are briefly presented in the following paragraph, according to the volcano-stratigraphy developed by Labarthe-Hernández et al. (1982; cf. Fig. 1).

The emplacement of the SLPVF began with the *Casita Blanca Andesite* which is composed of basaltic to andesitic lava flows of porphyric texture with ~5 vol. % of biotite and plagioclase phenocrystals; ages obtained for this unit are between 43.7 and 36.5 Ma (Tristán-González et al. 2009). The subsequent *Santa María Ignimbrite* yields welded ash-flow tuffs with 30 to 40 vol. % of mainly quartz and sanidine phenocrystals and collapsed pumice (Tristán-González et al. 2006; Tristán-González et al. 2009). The *Portezuelo Latite*, generated around 30.6 Ma,

consists of different lava flows with porphyric texture (30 vol.% of sanidine, albite and quartz phenocrystals). It overlies some Mesozoic marine formations with discordant contact and is stratigraphically followed by the *Panalillo Ignimbrite* (Tristán-González 1986). The latter unit is composed of two members with the inferior member consisting of pyroclastic flows filling small tectonic structures and the superior one of co-ignimbrite and welded ignimbrite; their age is between 26.8 and 28.0 Ma (Tristán-González et al. 2009). The *San Miguelito Rhyolite* was named after the outcrop of the lava flows in the Sierra de San Miguelito. This widespread unit is composed of highly viscous, topaz bearing lava flows that formed dome structures showing flow foliation, shrinkage fractures and tephra surges similar to structures reported from the U.S.A. by Christiansen et al. (1983). This rock has 5 to 20 vol.% of phenocrystals of quartz and feldspar in the devitrified matrix (Aguillón-Robles et al. 1994; Tristán-González et al. 2009). The *Cantera Ignimbrite* was described as a violet to gray coloured rock with 5 to 10 vol.% of phenocrystals (quartz and sanidine) and uncollapsed pumice. It is associated with the main volcanic event of the Sierra de San Miguelito. The *El Zapote Rhyolite* (not sampled for this study) represents the latest volcanic event of the Sierra de San Miguelito, and is composed of gray coloured lava flows with ~30 vol.% of phenocrystals (quartz, sanidine) and an isotopic age of 27.0 Ma (Nieto-Samaniego et al. 1996). Overall, the studied volcanic rocks are geochemically well differentiated (felsic to intermediate).

Expansive structures (mainly normal faults) bound a regional horst and graben structure and were used as conduits for volcanism (Tristán-González 1986). Based on geochemical variations, Orozco-Esquivel et al. (2002) divided the described succession into a lower and an upper volcanic sequence. The younger (upper) one consists of mainly rhyolitic lavas that contain topaz and are enriched in F and incompatible lithophile elements. This subdivision was adopted for geochemical interpretations in the present study (cf. chapter 3.1). The allocation of the sampled lithologies for the two sequences can be found in Table 1.

128 A clastic sequence of debris flow sediments containing volcanic material derived from the
129 weathering of the surrounding volcanic rocks syn-tectonically filled the graben structure as
130 basin-fill sediments. Calcareous material resulting from erosion of Cretaceous rocks in Sierra
131 San Pedro also contributed to these sediments and is inter-bedded with the pyroclastic
132 material; the total filling is referred to as Tertiary Granular Undifferentiated (TGU). Cardona
133 (2007) used information from borehole logging, resistivity surveys and lithology samples to
134 determine the general granulometric distribution and thickness of the basin filling. Depending
135 on the intra-graben position, the granulometric distribution varies from alluvial fan deposits to
136 playa sediments in the lowest topographical part of the graben structure. Depth to the Tertiary
137 fractured volcanic rocks beneath the basin fill sediments is about 250-300 m on average with
138 highest thicknesses of about 450-500 m in the northeastern region of SLP City.
139 Within the SLP City plain, two main hydrogeological units – I) shallow, and II) deep aquifer
140 – are vertically separated by a fine-grained layer with low hydraulic conductivity (ca. 10^{-11}
141 m/s). The shallow alluvial aquifer unit is unconfined while the deep aquifer unit is confined
142 below the mentioned fine-grained layer and unconfined elsewhere, being heterogeneous and
143 anisotropic in both fractured (volcanic rocks) and granular (TGU) material. Cretaceous
144 carbonate rocks represent the lower flow boundary.
145 Information presented by Carrillo-Rivera et al. (1996, 2002, 2007) and Cardona and Carrillo-
146 Rivera (2006) indicate the presence of two flow systems *sensu* Tóth (1998) in the deep aquifer
147 unit: IIa) a deep regional flow system represented by thermal water (35-40°C at borehole-
148 head); elevated B, F, Na and Li concentrations indicate interaction with fractured volcanic
149 rocks, and IIb) an intermediate shallow flow system with a temperature of 23-28°C and low
150 concentrations of B, F, Na and Li, indicating interaction with the basin fill sediments. Both
151 systems are ^{3}H free. Absolute age determinations using ^{14}C indicate that actually extracted
152 groundwater from the regional system is around 5,000-6,000 years old while the intermediate

153 system water shows ages of 2,000-3,000 years. Intensive water extraction was applied to the
154 top of the deep aquifer unit to supply the growing city for the 1977-2007 period. This resulted
155 in considerable groundwater table drawdown (ranging from 90 to 25 m) in deep (100 to 450
156 m below ground surface) boreholes following from an increase in total annual extraction from
157 1.9 to 4.1 m^3/s in the same period of time. As a consequence, old regional flow groundwater
158 started ascending to the production boreholes depth.
159
160 **1.3 Fluoride situation in SLP**
161 Dental fluorosis has been increasingly reported from the inhabitants of the city of SLP
162 (Carrillo-Rivera et al. 2002) and recognized as the result of high exposure to naturally
163 occurring F^- in the drinking water supply, a connection also observed in other parts of Mexico
164 (e.g., García-Pérez et al. 2013). This is causing some degree of dental fluorosis in 84 % of the
165 inhabitants between 6 and 30 years of age; 34 % of the 11 to 13 years old children showed
166 severe fluorosis (Medellín-Milán et al. 1993; Grimaldo et al. 1995). Severe dental fluorosis
167 was observed in children only, senior citizens lack significant effects (Sarabia 1989)
168 suggesting the former have been in contact with comparatively higher F^- concentrations in the
169 water supply than the latter users.
170 Tapped groundwater in 1987 for SLP city comprised various proportions of the aforementioned
171 shallow intermediate and the deep regional flow systems (Carrillo-Rivera et al. 2002). Mixing of
172 these flows takes place depending on extraction regime, local contrast in hydraulic
173 characteristics, and borehole construction, depth, design and operation. Maximum F^-
174 concentrations found in 1987 (3.7 mg/L) were argued to become higher still, in time and space,
175 should the input of regional F^--rich flow to the extraction boreholes be further enhanced. The
176 worst case scenario would be the extraction of 100 % of the deep regional flow component. It
177 was suggested that by controlling the extraction borehole-head water temperature at 28-30 ºC, an

178 extracted raw water mixture with F^- concentrations close to the maximum drinking water
179 standard of 1.5 mg/L could be obtained (Carrillo-Rivera et al. 2002).
180 Historical chemical analyses of regional flow groundwater (Stretta and Del Arenal 1960) show
181 remarkable temporal constancy in major ion hydrochemical composition. Field groundwater
182 temperature measurements exhibit a linear relationship to F^- concentrations which permits an
183 indirect estimation for the F^- concentration in extracted groundwater. Extraction rates increased
184 from ≈0.6 m^3/s in the 1960's to ≈2.6 m^3/s in 1987, thereby inducing vertical F^--rich water flow
185 into boreholes (in this paper understood as all ground perforations with pumping equipment for
186 the extraction of water serving for public supply) located in the centre of the SLP catchment.
187 Assessing the situation in 1987, regionalization of F^- concentrations in 52 groundwater samples
188 from boreholes distributed in the territories as represented in Figure 1 produced a surface area
189 affected by high F^- (>2 mg/L) of about 73 km^2. The contour map represented by the 2 mg/L F^-
190 isoline was delineated using linear kriging without any data transformation (model range: 7,483
191 m). The goodness of fit for the gridding method was calculated using residuals and the
192 coefficient of multiple determination (R^2). Results for 1987 data indicate a R^2 value of 0.996,
193 showing that in this case linear kriging is a suitable method as compared with e.g., polynomial
194 regression (R^2=0.401). The high F^- (>2 mg/L) surface area (135 km^2) determined for 2007 (107
195 groundwater samples) was delineated with the same gridding method. The higher sampling
196 density allowed a model range of 4,246 m, producing a R^2 value of 0.987. Comparison of F^-
197 concentration values for the eastern, southern and northeastern regions of the study area show no
198 major evolution in the 1987-2007 period with most concentrations below the drinking water
199 standard of 1.5 mg/L F^- (exceptions: territories associated with the boreholes D and H; Fig. 1).
200 Consequently, further increase in groundwater extraction enhanced the surface area affected by
201 high F^- (>2 mg/L) inflow from 73 km^2 in 1987 to 135 km^2 in 2007 (i.e. +85 %; Fig. 1).

202 At present, the estimated withdrawal is ≈4.1 m^3/s, additional boreholes are mainly tapping the
203 regional system at the foot of the felsic volcanic SSM to the west of the catchment. Additional F^-
204 attenuation methods in extraction boreholes should consider the hydrogeological and
205 geochemical control mechanisms of F^- as well as the borehole construction design to regulate the
206 percentage of different groundwater flows supplying an extraction borehole. The objectives of
207 this study are to characterize the primary F^- source, to evaluate natural F^- control under observed
208 increased groundwater extraction in the SLP catchment and to reassess F^- attenuation measures
209 as proposed under 1987 conditions.
210
211 **2 Materials and Methods**
212 **2.1 Water sampling and analyses**
213 Standard water sampling procedures included detailed field measurements of temperature,
214 pH, Eh, dissolved O_2 and electrical conductivity (APHA-AWWA-WPCF, 1989). An in-line
215 flow-cell at a by-pass of the standpipe was used to ensure exclusion of atmospheric
216 interference and to improve measurement stability. Two filtered (0.45 µm) samples were
217 taken at each site in acid-washed, well rinsed low density polyethylene bottles. One sample
218 for major cation and trace element determination was acidified with high purity HNO_3,
219 producing a pH of about 2, sufficient to stabilize trace metals. One filtered, un-acidified
220 sample was collected for anion analysis. Alkalinity was obtained through standard volumetric
221 Gran titration method using H_2SO_4 and a digital titration device. All used equipment was
222 calibrated *in situ*. Water samples were kept at 4°C before hydrochemical analysis. Chemical
223 solutions used during field determinations were subject to quality control. All reported values
224 have ionic balance errors within 5 %, except 5 out of 140 samples which show errors below
225 10 %. A complete suite of major (HCO_3^-, Cl^-, SO_4^{2-}, Ca^{2+}, Na^+, Mg^{2+}) and minor (NO_3^-, K^+, F^-
226) ions as well as some trace element (Li, Sr, Fe, Mn) analyses were conducted, although for

this investigation, only Li (atomic adsorption spectroscopy) and F (ion selective electrode) were considered for the interpretation of hydrochemical data. Water analyses were carried out at the Soil and Water Chemical Laboratory of the Engineering Faculty of the UASLP.

2.2 Rock sampling and analyses

Sampling of the volcanic rocks was done considering the stratigraphic volcanic sequence determined by Labarthe-Hernández et al. (1982), six out of the eight most representative volcanic units were sampled (8 samples) in different locations. In addition to own sampling and analysis, volcanic rock chemical data were taken from previous studies in the area (Orozco-Esquivel et al. 2002; Rodríguez-Ríos 1997) to extent the geochemical database to a total of 38 samples (1 andesite, 1 latite, 4 rhyolitic ignimbrite, 32 rhyolite samples) with a strong focus on rhyolites accounting for the dominance of this rock type in the study area. Whole rock samples were analyzed for major elements using a Siemens SRS 3000 X-ray sequential spectrometer. The determination of trace elements was done by ICP-MS (Perkin Elmer ELAN 9000).

Three thin sections were produced from rhyolite samples (San Miguelito Rhyolite) of different alteration grades and studied under the microscope (Olympus IX70) using transmitted light and an ultraviolet lamp for the identification of F-bearing minor mineral phases. Aliquots of those three rhyolites were ground to powder grain size (McCrone corundum mill) and analyzed for their mineralogical composition using a Bruker AXS D8 Advance X-ray diffractometer (CuKα radiation; operational adjustments: 40 kV, 40 mA, 2θ = 2-92°). The proportion of amorphous glassy material in the samples was estimated by adding an internal anatase standard (10 wt. % of total sample size).

2.3 Processing of analytical information

Available data on the physical and hydrochemical behavior of groundwater when flowing through different lithologies of the SLP region were interpreted based on the flow system theory (Tóth 1998) from where the hierarchy of different flow systems (local, intermediate and regional) have been defined with the combined use of additional geographical data (i.e., geomorphology, soil and vegetation) suggesting the existence of recharge, transit or discharge conditions. The conceptual contrasting biophysical differences, among others, of the different hierarchical flow systems assembled by Tóth (1998) allow to propose – above basic groundwater flow – systems that move individually under natural conditions. This characterization has proved to be applicable in the study area (Carrillo-Rivera et al. 2002, 2007). Under natural conditions, local flows have the shortest travel depth and distance, and contain groundwater with temperature closest to that of the recharge environment; therefore, this sub-recent water has comparatively low pH and total dissolved solids (TDS); its dissolved oxygen (DO) concentration is high. In contrast, the regional flow will travel the deepest and longest paths, achieving a water temperature and TDS as functions of depth and distance of travel. The pH of the water will increase, and its DO decrease, it represents the oldest water in the system. An intermediate flow system can be developed between local and regional systems. In the study area, local flows are ephemeral showing their presence only during the rainy season; therefore the next flow in the hierarchical position is the one of intermediate nature. Regional flow has been shown to be characterized by the highest temperature, Li and F^- concentrations, due to its deepest travelling path and nature of the hosting felsic rock units; whereas intermediate flow has lower temperature as well as lesser Li and F^- concentrations (Carrillo-Rivera et al. 2002). Using the hydrogeochemical modeling software Phreeqc (Parkhurst et al. 1980) allowed for the evaluation of water-mineral equilibria and mixtures between the identified flows.

276 Statistical analysis of the geochemistry dataset was conducted using the software SPSS
277 Statistics 17.0. Quantification calculations of mineral phases after XRD determinations were
278 conducted applying Rietveld analysis with the software BGMN, version 4.2.3.
279
280 **3 Results and Discussion**
281 **3.1 Geochemical and mineralogical characterisation of the fluoride source**
282 Geochemical data obtained from own analyses and previous studies (Orozco-Esquivel et al.
283 2002; Rodríguez-Ríos 1997) are presented in Table 1. Separation between Lower and Upper
284 volcanic sequence was adopted as suggested by Orozco-Esquivel et al. (2002).
285
286 **Table 1**: Selected geochemical data of volcanic rocks from the study area and its vicinity (own analyses and data
287 from Orozco-Esquivel et al. 2002 and Rodríguez-Ríos 1997). ACB: Casita Blanca Andesite, LP: Portezuelo
288 Latite, ISM: Santa María Ignimbrite, IC: Cantera Ignimbrite, IP: Panalillo Ignimbrite, RSM: San Miguelito
289 Rhyolite, RS: Santana Rhyolite, RC: Carbonera Rhyolite, R: rhyolites from different domes and flows, RL:
290 Lower sequence rhyolites, RU: Upper sequence rhyolites.

Strati-graphy	Sample	Si	Al	Fe	Ca	Mg	Na	K		F	Rb	Sr	Zr	Nb	Ba	La	Eu	Yb	Ta	Th
		wt. %								µg g^{-1}										
Upper sequence																				
IC	M-5	35.7	6.6	0.8	0.0	0.1	2.0	4.4		608	272	32	147	30	203	27.6	0.5	7.3	2.0	25
	M-6	35.5	6.7	0.9	0.3	0.0	2.4	4.2		595	269	46	166	29	318	57.6	0.5	5.3	1.9	39
IP	M-8	35.5	6.9	1.1	0.1	0.0	2.5	4.1		116	251	9	300	53	62	61.9	0.3	8.0	3.1	40
SSM	M-7	35.9	6.5	1.2	0.2	0.0	2.2	4.1		2651	594	7	139	44	64	25.5	0.1	8.5	4.2	79
	M-9	35.3	6.8	1.1	0.1	0.0	2.4	4.0		1032	375	18	151	32	258	32.3	0.2	6.3	2.8	46
	CG/95/3	31.9	7.4	2.4	0.7	0.0	1.2	4.8		2100	484	6	137	34	17	37.1	0.1	4.5	5.1	55
	CG/95/4	31.8	7.3	2.8	0.6	0.1	1.1	4.6		1900	499	8	135	36	43	24.7	0.1	5.4	5.3	37
	CG/95/5	32.1	7.2	2.8	0.6	0.1	1.1	4.4		3500	479	7	134	32	22	67.9	0.1	13.2	4.8	62
	CG/95/7	36.4	6.1	1.0	0.3	0.0	1.7	4.7		1700	399	9	141	25	34	20.8	0.1	3.6	3.4	38
	CG/95/9	34.5	6.8	1.8	0.2	0.0	1.5	4.8		2400	75	10	127	33	62	11.7	0.1	5.7	5.0	46
	CG/95/49	34.2	6.4	2.4	0.2	0.0	1.2	5.6		2500	471	12	130	34	62	13.3	0.1	3.3	5.0	45
	CS/95/10	34.7	6.5	1.6	0.6	0.0	1.4	4.8		600	262	27	160	19	276	68.4	0.3	5.1	2.2	34
	CS/95/11	35.1	6.9	1.8	0.5	0.0	1.9	4.6		1000	265	17	124	20	101	50.2	0.2	5.6	2.5	33
	CS/95/12	35.3	6.7	1.4	0.5	0.0	1.9	4.0		800	275	27	125	21	625	46.5	0.2	4.9	2.5	33
	CS/95/14	35.6	6.2	1.6	0.6	0.0	1.9	4.2		2500	432	8	131	29	77	13.3	0. 1	6.0	4.2	36
RS	DS/96/2	36.4	6.0	1.0	0.2	0.4	1.4	4.1		540	316	100	248	17	705	41.0	0.8	2.0	2.1	20
	DS/96/3	36.2	6.0	1.0	0.3	0.5	2.0	4.0		1600	317	100	266	19	747	58.8	1.1	3.3	2.3	21
	DS/95/28	36.2	5.9	0.9	0.2	0.4	1.9	4.0		1200	248	100	228	17	611	47.6	1.1	3.5	1.8	21
RC	DS/95/22	35.6	6.4	1.3	0.1	0.0	2.1	3.9		410	290	32	213	21	283	53.6	0.5	5.9	2.7	28
	DS/95/45	33.3	7.1	3.3	1.2	0.0	2.1	4.2		170	221	24	387	37	341	100	1.0	7.3	3.0	24
	DS/96/1	33.6	7.0	2.5	1.6	0.1	2.2	4.2		340	254	112	275	20	851	74.0	1.1	3.0	2.1	22
R	RIO-16	35.5	6.9	1.0	0.4	0.1	2.5	4.5		7603	581	6	125	42	50	75.8	0.2	19.2	6.2	85
	RIO-12	35.6	7.0	1.0	0.3	0.1	2.1	4.6		1463	407	9	113	19	28	17.9	0.1	5.5	3.9	36
	RIO-9	35.9	6.8	1.1	0.2	0.1	2.0	4.1		1289	307	9	86	24	49	10.0	0.1	6.2	3.2	30

	RIO-44	35.9	6.7	1.0	0.2	0.1	2.5	4.0		2840	601	7	143	30	89	24.3	0.1	5.0	5.5	57
	RIO-41	36.3	6.5	0.9	0.3	0.1	1.9	4.2		1296	359	8	144	23	20	21.7	0.1	5.2	3.3	33
	RIO-46	36.5	6.2	0.8	0.4	0.1	1.9	4.2		1149	330	9	112	18	49	35.3	0.1	7.2	2.9	28
	RIO-43	36.6	6.2	0.9	0.4	0.1	1.9	4.2		1039	322	13	145	17	70	28.7	0.2	6.0	2.7	32
	RIO-7	36.3	6.6	1.0	0.1	0.1	1.5	4.0		356	186	20	113	16	137	19.6	0.3	3.9	1.7	16
Ø RU		35.1	6.6	1.5	0.4	0.1	1.8	4.3		1691	359	27	162	26	218	39.3	0.3	6.0	3.5	38
Ø RSM		34.4	6.7	1.8	0.4	0.0	1.6	4.6		1890	384	12	136	29	136	34.3	0.1	6.0	3.9	45
Lower sequence																				
ACB	M-1	25.5	8.7	6.2	5.4	2.5	2.5	1.5		1005	47	572	322	14	684	39.0	1.9	2.4	0.7	6
LP	M-4	31.4	6.7	3.8	2.9	0.2	2.0	3.7		592	199	205	380	24	2371	77.7	1.9	6.3	1.9	18
ISM	M-2	35.4	5.9	2.4	0.7	0.1	1.8	4.2		358	189	98	234	22	1346	50.7	1.1	3.5	1.3	24
R	RIO-45	33.3	7.1	3.3	1.2	0.2	2.1	4.2		1082	189	141	501	18	1340	53.6	1.7	4.5	1.8	17
	RIO-29	33.6	7.0	2.5	1.6	0.2	2.2	4.2		1336	159	129	457	16	1630	59.0	1.6	4.8	1.9	16
	RIO-22	34.7	6.5	1.6	0.6	0.3	1.4	4.8		322	193	62	278	13	1300	61.2	1.1	4.6	1.8	18
	RIO-18	35.1	6.9	1.8	0.5	0.2	1.9	4.6		250	170	91	277	13	1480	61.6	1.3	4.4	1.7	16
	RIO-47	35.3	6.7	1.4	0.5	0.1	1.9	4.0		207	181	78	304	14	1410	77.8	1.4	5.7	1.5	18
	RIO-24	35.6	6.2	1.6	0.6	0.1	1.9	4.2		489	155	90	250	15	1360	53.5	1.2	3.9	1.8	19
Ø RL		34.6	6.7	2.0	0.8	0.4	1.9	4.3		614	174	98	344	14	1420	61.1	1.4	4.7	1.8	17
Ø RU/ Ø RL		1.01	0.98	0.75	0.51	0.25	0.95	1.00		2.75	2.06	0.27	0.47	1.76	0.15	0.64	0.23	1.28	1.99	2.21
Ø RSM/ Ø RL		0.99	1.00	0.90	0.50	0.00	0.85	1.05		3.08	2.20	0.13	0.40	2.01	0.10	0.56	0.10	1.29	2.24	2.62

Major ion contents in rhyolites from both sequences are relatively stable, average values are very similar (Table 1) with the exception of calcium which is depleted in the Upper sequence, compared to the Lower one. With an average content of nearly 1,700 µg g^{-1}, F in Upper sequence rhyolites is enriched by a factor of 2.75 compared to Lower sequence rhyolites. This trend is even more pronounced in rhyolites from the Sierra San Miguelito (Ø nearly 1,900 µg g^{-1} F; enrichment factor 3.08). For comparison, average F content in acid igneous rocks is 800-1,000 µg g^{-1} (Lucas 1988). Fluorine enrichment in the Upper sequence occurs together with some incompatible large ion lithophile elements (LILE: Rb, Cs, Heavy REE, U, Th, Pb) and high field strength elements (HFSE: Nb, Ta) as shown by enrichment factors in Table 1 and correlation coefficients with F in Fig. 2d. In contrary, feldspar-compatible elements (Ba, Sr, Eu), Zr and Light REE are depleted in the Upper sequence. Both observations suggest F being hosted in late magmatic mineral phases or the matrix. These findings are in good agreement with the results of Orozco-Esquivel et al. (2002) indicating the regional rhyolites´ geochemical similarity to rhyolites from the western U.S.A. (Christiansen et al. 1983). This

underlines the incompatible behavior of F and thus its tendency to be concentrated in the melt fraction during magmatic differentiation (e.g. Stecher 1998). Similar to F behavior, all mentioned enrichment and depletion trends of other elements are even more distinct when only Sierra San Miguelito rhyolites are taken into account (Table 1). Figures 2a-c illustrate F scatter plots versus different elements, with samples being differentiated between Upper and Lower volcanic sequence.

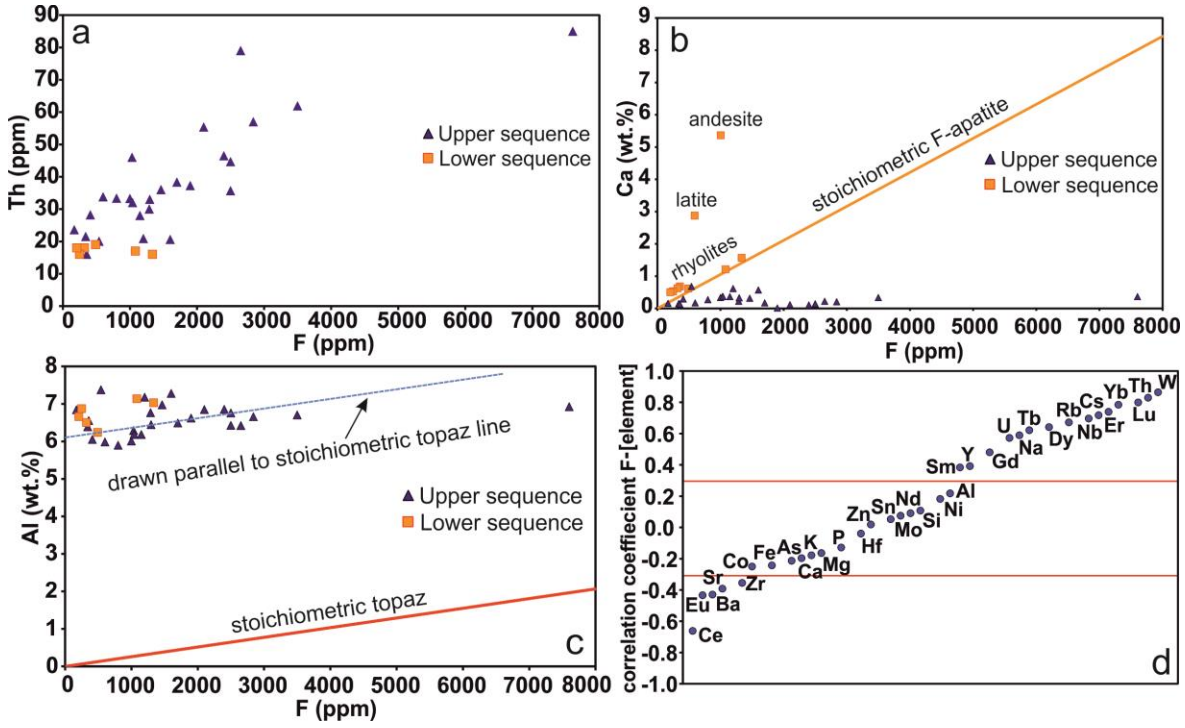

Fig. 2: Fluorine correlation with other elements in studied volcanic rocks; a: F-Th scatter plot, b: F-Ca scatter plot, c: F-Al scatter plot, d: Pearson correlation coefficients F-[element] for all rhyolite samples, lines indicating distinct positive ($R^2 \geq 0.3$) and negative ($R^2 \leq -0.3$) correlation.

As an example for flourine enrichment and occurrence together with incompatible elements, Figure 2a shows a positive correlation ($R^2=0.69$) between F and Th in the Upper sequence while no relation is observable in Lower sequence rhyolites. Figure 2b contains the stoichiometric F/Ca ratio of fluorapatite $Ca_5(PO_4)_3F$ with Lower sequence rhyolites closely ($R^2=0.98$) following this line (andesite and latite represent outliers with substantial excess

Ca), while Upper sequence rhyolites developed differently, acquiring excess F. This suggests that fluorapatite controls the F budget of the Lower sequence rhyolites while it is of lesser importance for the Upper sequence. The stoichiometric F-Al ratio of topaz $Al_2(SiO_4)F_{1.1}(OH)_{0.9}$ was implemented in Fig. 2c to evaluate the importance of this mineral phase for F distribution. In this diagram, Upper sequence rhyolites scatter subparallely to the topaz line (with large excess of Al caused by feldspar presence). This indicates F being at least partly bound in topaz, especially in the Upper sequence as reported by Orozco-Esquivel et al. (2002).

Quantitative X-ray diffraction results obtained by Rietveld analysis are presented in Fig. 3. Sample (a) represents an unweathered rhyolite while (c) is a more altered sample (with (b) being intermediate between (a) and (c)) as concluded from observation of rather grayish colour and decreasing consolidation of the latter. This is supported by mineralogical results showing a decrease of comparatively well weatherable plagioclase and biotite and an increase of the weathering product kaolinite (Fig. 3).

	quartz	sanidine	plagioclase	kaolinite	biotite	zircon	corundum	topaz	F-apatite	stoichiometric topaz-F	stoichiometric apatite-F
(a)	25.87	25.50	34.43	1.96	6.18	0.74	2.76	1.58	1.15	0.182	0.044
(b)	26.16	31.86	29.15	2.62	5.73	0.50	1.46	1.46	1.04	0.167	0.039
(c)	27.95	31.21	25.48	5.00	4.57	0.60	1.24	2.27	0.78	0.260	0.030

Fig. 3: Microscopic images and mineralogical composition of rhyolites, and F contents calculated for identified F-bearing mineral phases (in wt. %) in samples (a), (b) and (c) from Sierra San Miguelito (SSM).

343 The anatase standard material was not overestimated in the Rietveld quantification, indicating
344 that there is no significant proportion of X-ray amorphous material in the samples.
345 Nevertheless, it cannot be excluded that background intensity is partly taken by fitted
346 minerals, as indicated by broadened reflexes of some phases, which may lead to
347 underestimation of the standard and thus represents a potential source of quantification
348 uncertainty. The proportional scale and trends between the samples are, however, considered
349 trustworthy. Topaz and F-apatite were identified as F-bearing mineral phases while fluorite
350 has not been detected. Stoichiometric bulk rock F contents were calculated from the Rietveld
351 data (Fig. 3). The values plot in the range of the typical F content of San Miguelito rhyolites
352 (Table 1). As suggested by element correlation analysis (Fig. 2c), topaz is the main F host
353 mineral in these rocks. Nevertheless, the availability of topaz-F to be desintigrated into its
354 sorrounding environment is rather limited due to the high resistance to weathering of this
355 mineral. This is supported by topaz content being highest in the most altered rhyolite sample
356 (Fig. 3). In contrast, F-apatite successively decreases with increasing alteration indicating that
357 this mineral, despite its lower abundance, may be the more important F^- source in terms of
358 remobilization and release into groundwater. Apatite weathering is heavily temperature-
359 dependent (Guidry and Mackenzie 2000) and may be triggered under the given warm and
360 semiarid climate of the study area, and especially under thermal water conditions. These
361 findings also suggest that rhyolites of the Lower volcanic sequence are potentially effective F^-
362 sources, despite their lower bulk F contents (Table 1, Fig. 2b).
363
364 **3.2 Dissolved fluoride development and hydrochemistry**
365 Figure 1 shows the region with F^- concentrations >2 mg/L in extraction boreholes for 1987
366 and 2007 data. A comparison of these two datasets suggests that the new boreholes
367 constructed to the NW and S of SLP City are under the influence of high F^- water. These

368 boreholes are located directly on the felsic volcanic material, they tap the regional flow
369 without any further possible control. However, F^- concentrations in other parts of the city area
370 remained similar to values reported for 1987 (Carrillo-Rivera et al. 2002).
371 The relation between groundwater temperature and its F^- concentration for 1987 and 2007
372 data (Fig. 4) suggests that an acceptable water quality (in terms of $F^- < 1.5$ mg/L) may be
373 obtained by keeping the extracted raw water mixture below a temperature of ~30°C.
374 Exceptions from this approach are represented by those boreholes with groundwater
375 extraction inducing intermediate flow water travel through the volcanic material which
376 produces an excess in F^- in extracted water (data above the R^2=0.8 trendline, i.e. boreholes
377 located in the framed fields in Fig. 4 with >1.5 mg/L F^-). Usage of these waters for drinking
378 purposes requires an individual F^- management. Nevertheless, should other influences be
379 absent in extraction boreholes, the control of discharge temperature at ~30 °C or lower may
380 keep F^- concentrations within satisfactory limits.
381

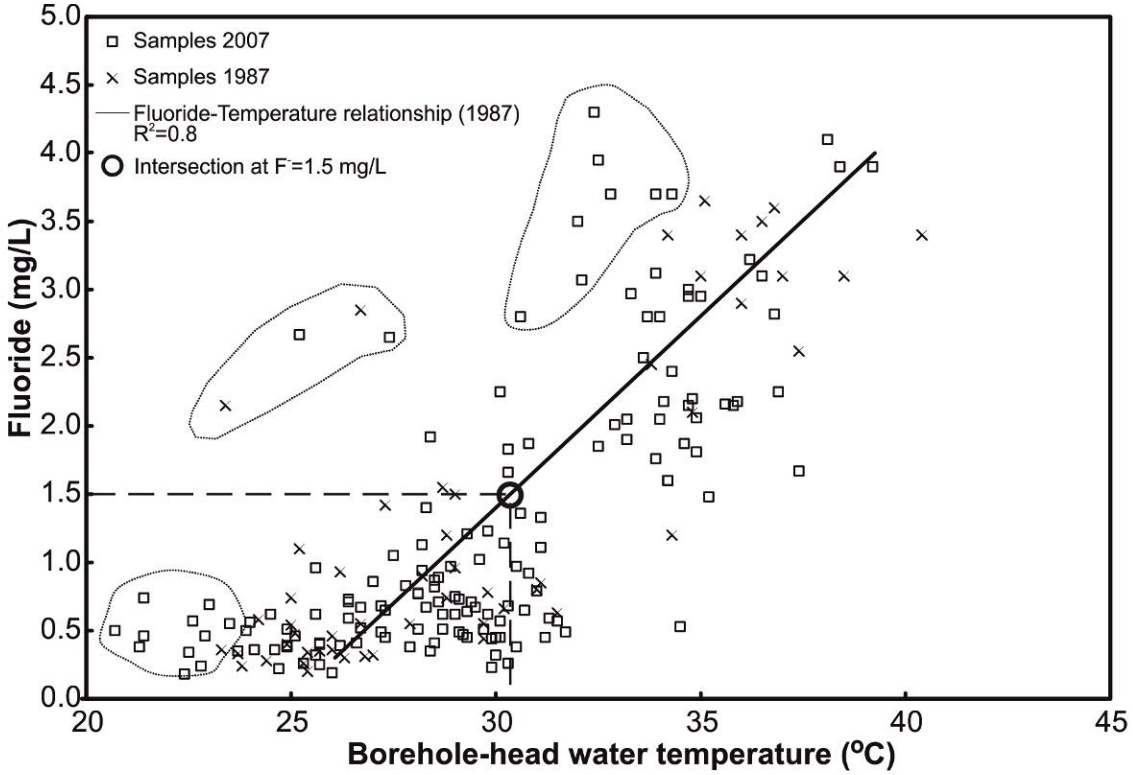

382

Fig. 4: Water discharge temperature *vs.* fluoride concentration for 1987 and 2007 samples. Framed fields mark sample groups with F^- concentrations significantly in excess of the displayed F^-/temperature relation.

Figure 5 indicates the relation between borehole discharge water temperature and F^- concentration in selected extraction boreholes, comparing 1987 and 2007 data (Table 2). Reduced extracted water temperature (solid line) for measurements made at boreholes A, B and C imply that inflow water changed along the mixture path resulting in a decreased F^- concentration. Other boreholes show a slight decrease in F^- but some increase in temperature (boreholes D, E, F, G, H, and I). Groundwater relative age, i.e. residence time, in terms of Li concentration appears to be similar in most of these cases (Table 2). Lithium concentrations in groundwater are controlled by water/rock interaction processes, mainly via release of Li during silicate weathering (Négrel et al. 2012). This metal is typically associated to felsic rocks like rhyolites and pegmatites due to its incompatibility during magmatic differentiation (e.g., Benson et al. 2017). Edmunds and Smedley (2000) observed positive correlation of Li with groundwater temperature as well as with ^{14}C age, and used the element as an indicator of groundwater residence time. It was also successfully used to discriminate between thermal and shallow groundwater (Carrillo-Rivera et al. 1996; Lambrakis et al. 2013).

New boreholes (I, J, K, L) have been constructed close to sites where old boreholes were removed due to a deteriorating extraction regime. Data for the old borehole (1987) as compared to the new site (2007) put forward that the proposed mixture line for the 1987 data (cf. Carrillo-Rivera et al. 2002) is still valid (Table 2, Fig. 5).

Table 2: Temperature, lithium and fluoride results for groundwater samples from 1987 and 2007 (T given in °C, Li and F concentrations in mg/L).

Borehole	T (1987)	T (2007)	ΔT (2007-1987)	Li (1987)	Li (2007)	ΔLi (2007-1987)	F (1987)	F (2007)	ΔF (2007-1987)
A	37.4	29.1	-8.3	0.17	0.08	-0.09	2.55	0.49	-2.06
B	29.0	24.1	-4.9	0.12	0.01	-0.11	0.96	0.36	-0.60
C	28.7	28.3	-0.4	0.10	0.11	0.01	1.55	1.40	-0.15

D	26.7	27.4	0.7	0.07	0.07	0.00	2.85	2.65	-0.20
E	35.1	36.5	1.4	0.18	0.20	0.02	3.65	3.10	-0.55
F	36.0	36.8	0.8	0.18	0.18	0.00	2.90	2.82	-0.08
G	24.2	24.9	0.7	0.04	0.03	-0.01	0.58	0.51	-0.07
H	34.8	35.2	0.4	0.15	0.15	0.00	2.10	1.48	-0.62
I*	33.8	35.6	1.8	0.17	0.17	0.00	2.45	2.16	-0.29
J*	40.4	29.0	-11.4	0.22	0.05	-0.17	3.40	0.62	-2.78
K*	27.0	35.9	8.9	0.03	0.19	0.16	0.32	2.18	1.86
L*	25.2	30.6	5.4	0.04	0.13	0.09	1.10	2.80	1.70
M	25.4	24.6	-0.8	0.01	0.01	0.00	0.20	0.36	0.16
N	38.5	36.2	-2.3	0.18	0.18	0.00	3.10	3.22	0.12
O	29.7	29.5	-0.2	0.05	0.02	-0.03	0.55	0.67	0.12
P	28.2	29.6	1.4	0.04	0.05	0.01	0.90	1.02	0.12

* New boreholes (2007 data) constructed near the old borehole sites (1987 data)

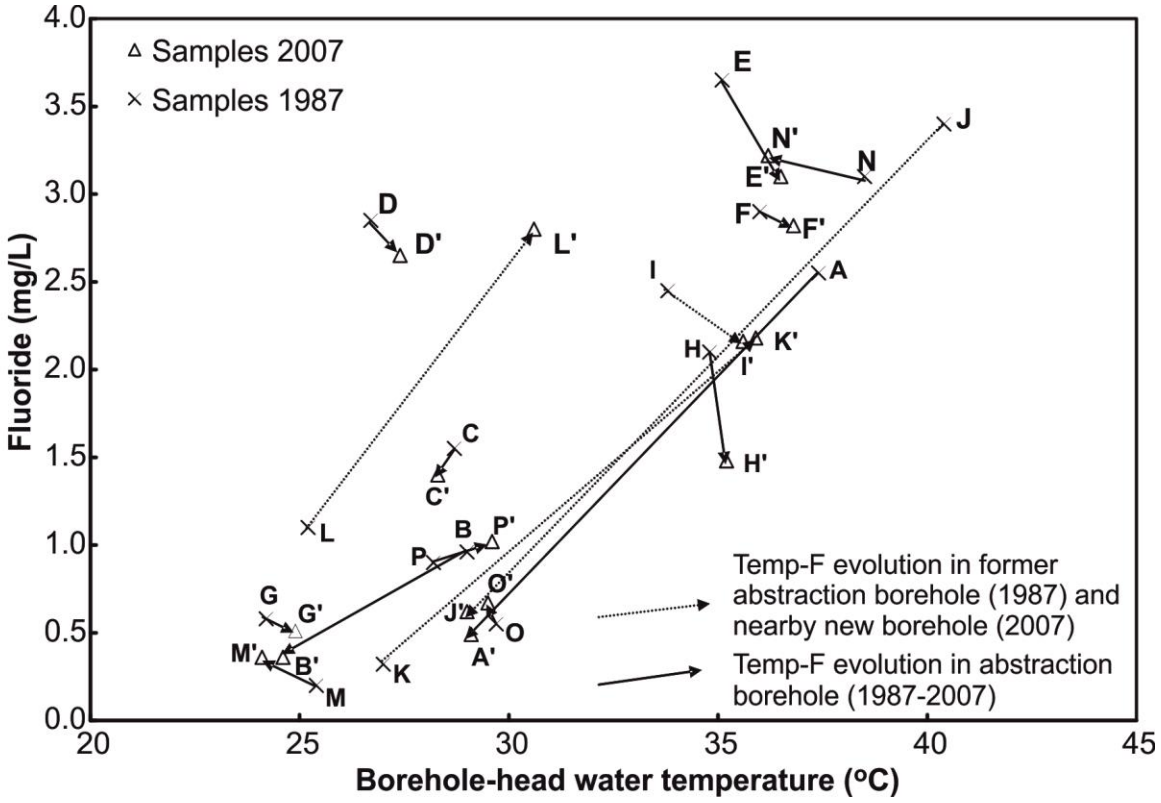

407

408 **Fig. 5**: Comparison of water discharge temperature *vs.* fluoride concentration for selected boreholes for 1987 and

409 2007 data.

410

411 Figure 6 directly visualizes the impact of temperature changes on the variations of F^- (Fig. 6a)

412 and Li (Fig. 6b) concentrations in groundwater, emphasising that both parameters can be

413 regarded as functions of groundwater temperature with R^2=0.84 for F^- and 0.91 for Li.

414

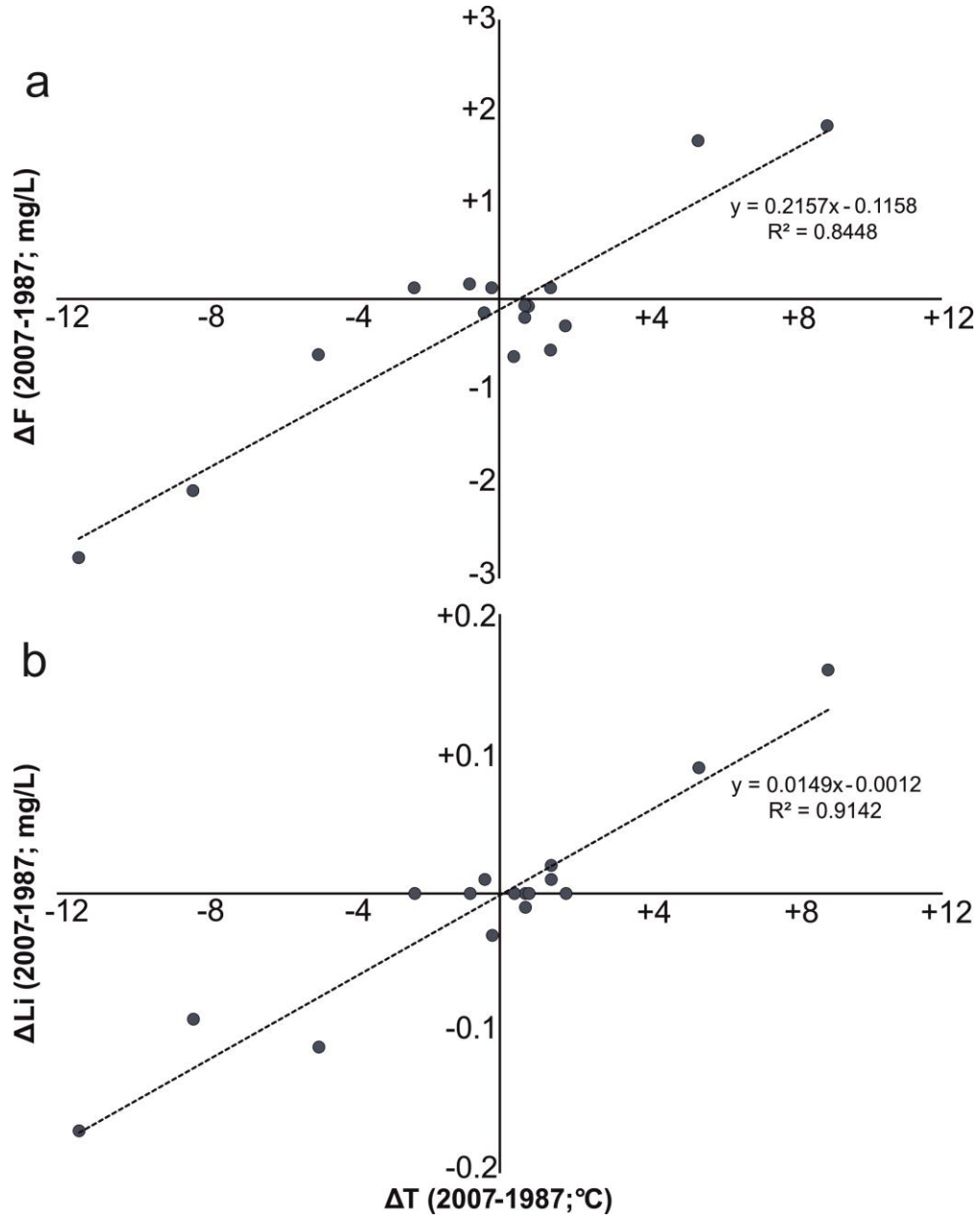

Fig. 6: Relation of groundwater temperature changes from 1987 to 2007 *vs.* changes in F^- (a) and Li (b) groundwater concentrations in the same period of time.

Natural F^- controls derived from 1987 data (Carrillo-Rivera et al. 2002) seem applicable to previous as well as new boreholes. As Li is expected to behave in a conservative manner, this property might be used to propose possible reactions relating F^- along the groundwater flow path to the extraction borehole. Figure 7 was constructed with boundaries for different cases that could be anticipated based on the nature of Li as water age indicator (Edmunds and

Smedley 2000) as well as with further support by the discharge temperature of the regional flow (33.8 to 40.4 °C), and that of intermediate flow (25.5 ± 1 °C), respectively. Assuming that the relationship between temperature values and F^- concentration has prevailed, from Fig. 4 and/or from the equation relating groundwater temperature (T) to its F^- concentration [F = (T-25.005)/3.562], samples depict the mixing end-members of cases (d) and (e) (Carrillo-Rivera et al. 2002). Figure 7 suggests that also more recent extraction induces water from the regional flow system, often with higher Li concentration implying longer residence time (Edmunds and Smedley 2000), and higher temperature than in the 1987 situation (*case d*). *Case a* represents the mechanical mixture between thermal and cold water end members (regional *(case d)* and intermediate *(case e)* flows). Data presented in Figure 7 suggests that a large number of boreholes is affected by mixed waters of different Tóthian groundwater flow system origin represented by *case a*. Fluoride increase (from 1987 to 2007) of borehole K (Fig. 5) is explained by the increase of the regional flow portion in the mixture with intermediate flow. Conversely, F^- reduction of borehole J is explained by an additional input of the intermediate flow end member with lower F^- and Li concentrations (Table 2).

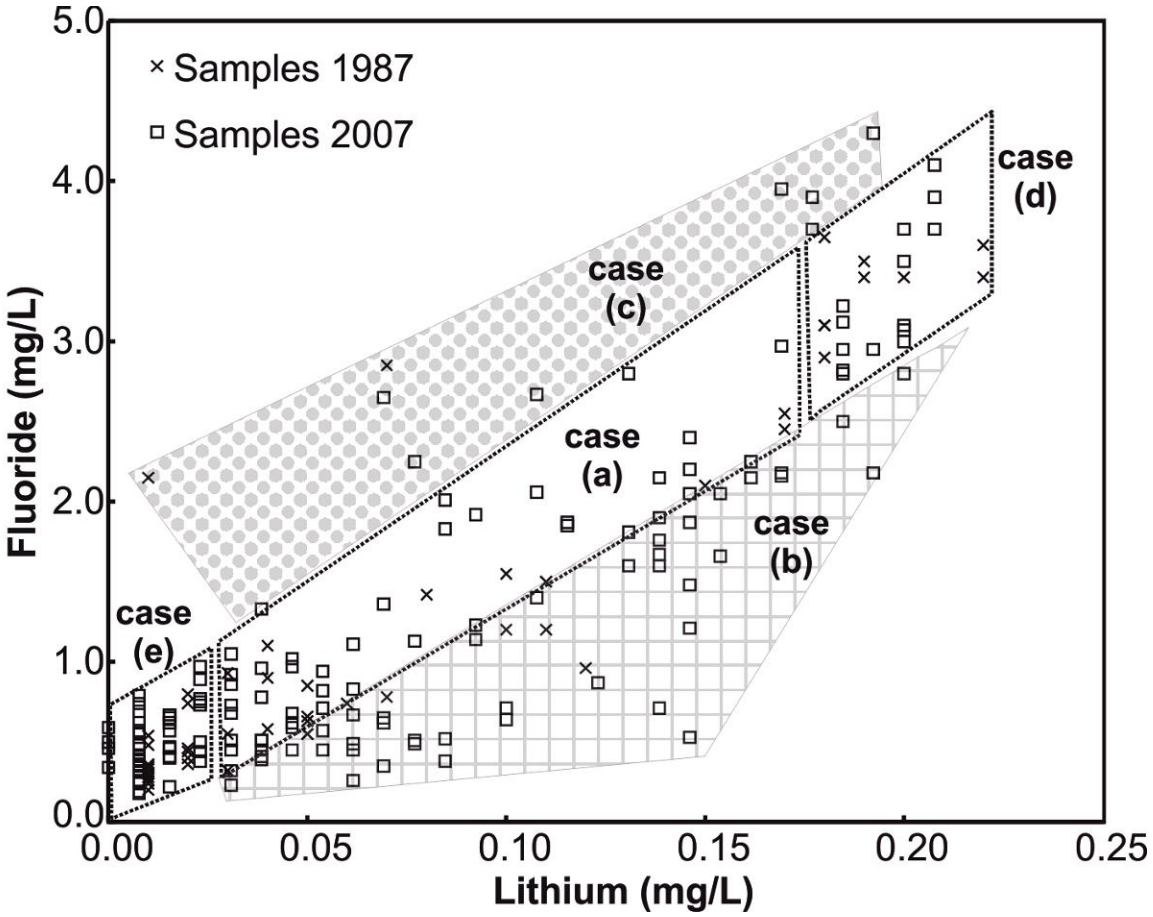

441

442 **Fig. 7**: Relation of Li (residence time indicator) *vs.* F^- for 1987-2007 data, showing F^- control cases (a) by
443 mixture, (b) reduction by precipitation, (c) F^- increase from sources in addition to regional flow, (d) high F^-
444 source (regional flow) and (e) low F^- source (intermediate flow).

445

446 *Case b* shows the effect of fluorite precipitation accompanied by reduced F^- concentrations in
447 the aqueous phase, as these samples, concluding from their 1987 position, would be expected
448 to belong to *case a* if only pure conservative mixing occurred. The solubility control by CaF_2
449 and associated loss of dissolved F^- in the water mixture when it travels through the Ca-rich
450 granular material ($CaCO_3$ containing sediments in the SLP graben basin) are plausible
451 possibilities to explain F^- reduction suggested by *case b*. Fewer samples represent *case c*; they
452 indicate fluoride input to groundwater from other sources in addition to the regional flow end
453 member.

Phreeqc calculations of saturation indices (Carrillo-Rivera et al. 2002) suggest that F^- concentration in the water of the regional flow system is controlled by fluorite solubility irrespective of extraction groundwater temperature. Calculations made using geothermometry proposed that this water attains a temperature of about 75°C at depth (at about 1,000-1,500 m) and that it is about in equilibrium with respect to fluorite (and calcite). Extracted groundwater (at discharge temperature) is under-saturated with respect to fluorite. Such results are interpreted as a F^- loss occurring in the ascent of regional flow water to borehole discharge. A natural F^- concentration control may be postulated by increasing calcium and lowering water temperature, which is feasible as the thermal water at borehole head is calcite under-saturated (or near equilibrium). Since fluorite over-saturation is not anticipated, the application of this solubility control is recommended for natural F^- reduction in future groundwater extraction schemes. Specific borehole design taking the geological and hydrogeological conditions into consideration may allow groundwater from the regional flow system to circulate through the Ca-rich granular material to trap dissolved F^- prior to extraction. Consequently, the application of the proposed *in situ* controls of F^- attenuation by the hydrogeological environment through response and travelling path of the groundwater flow systems may be favored over conventional treatment plants which would result in higher costs due to the substantial initial capital investment of such plants. Furthermore, their dimensioning and performance are unclear, they might be inefficient due to the observed evolution in water quality with extraction time as a function of variation in the extraction rate of intermediate/regional inflow to the borehole. Dependent on the selected water treatment approach, an additional environmental and financial concern would be the management of accumulating sludge.

There is a need for a better understanding regional flow systems by borehole drillers and borehole operators. Screens and discharge yield through step drawdown tests should be designed to tap more raw water from vertical flow, i.e. groundwater which reacted with Ca-rich aquifer

sediments to precipate F^- as CaF_2 before extraction. Raw waters with temperatures above the derived temperature control (30 °C) should be avoided or cooled down – ideally in the borehole – by appropriately controlling pumped water velocity for extra cooling time. These measures possibly come at the expense of higher capital expenditures (CapEx) but will be much cheaper than treatment of raw water for F^- removal. The latter should not be first choice due to (i) substantial operational expenditures (OpEx) adding to the CapEx, (ii) the need for trained people to run the plants adapting to changing raw water composition as discussed before, and (iii) the disperse water supply infrastructure which will require numerous treatment plants or a wide transport pipe network, both of which are hardly feasible.

4 Conclusions

Elevated F^- concentrations in groundwater around San Luis Potosí City were shown to primarily derive from geogenic mobilization of F-bearing mineral phases present in the surrounding felsic volcanic rocks. The natural F^- control mechanisms in the different Tóthian flow systems proposed in this study appear to be managing the presence and distribution of F^- in extracted groundwater in the SLP catchment. Data for 1987 and 2007 further suggests that the previously proposed counteractive measures (Carrillo-Rivera et al. 2002) *before* water is extracted are applicable and that it is advisable to fully consider them when new boreholes are constructed as well as in the management of existing ones as the efforts to remove F^- once it reaches the surface are costly and environmentally critical.

The proposed model and F^- controls could have wider applicability in similar hydrogeological frameworks in other parts of Mexico, the U.S.A. and the world, where groundwater derived from different Tóthian flow systems in a particular mixture is obtained for consumption in the growing number of recognized areas affected by elevated F^- concentrations.

5 Acknowledgments

Funding to carry out the present investigation was provided by Project FMSLP-2005-C01-10 by CONACyT and COTAS of San Luis Potosí Aquifer. Groundwater sampling for 2007 data was carried out by Thomas Hergt, Elias Nuñez and J. Ezequiel Escamilla; water analyses were performed by the Soil and Water Chemical Laboratory Staff of the Engineering Faculty of the UASLP.

6 References

Aguillón-Robles A, Aranda Gómez JJ, Solorio-Munguía JG (1994) Geología y tectónica de un conjunto de domos riolíticos del Oligoceno medio en el sur del Estado de San Luis Potosí, México. Rev Mexic Cienc Geol 11(1):29-42

Amini M, Mueller K, Abbaspour KC, Rosenberg T, Afyuni M, Møller KN, Sarr M, Johnson CA (2008) Statistical Modeling of Global Geogenic Fluoride Contamination in Groundwaters. Environ Sci Technol 42:3662-3668

APHA-AWWA-WPCF (ed., 1989) Standard methods for the examination of water and wastewater, vol 17. Washington, DC

Banning A, Rüde TR (2015) Apatite weathering as a geological driver of high uranium concentrations in groundwater. Appl Geochem 59:139-146

Benson TR, Coble MA, Rytuba JJ, Mahood GA (2017) Lithium enrichment in intracontinental rhyolite magmas leads to Li deposits in caldera basins. Nature Commun 8:270

Bjørklund G, Christophersen OA, Chirumbolo S, Selinus O, Aaseth J (2017) Recent aspects of uranium toxicology in medical geology. Environ Res 156:526-533

527 Cardona A, Carrillo-Rivera JJ (2006) Hidrogeoquímica de sistemas de flujo intermedio que
528 circulan por sedimentos continentales derivados de rocas riolíticas, Ingeniería Hidráulica en
529 México XXI(3):69-86

530 Cardona A (2007) Hidrogeoquímica de sistemas de flujo, regional, intermedio y local
531 resultado del marco geológico en la Mesa Central: reacciones, procesos y contaminación.
532 Dissertation UNAM, Mexico City

533 Carrillo-Rivera JJ, Cardona A, Moss D (1996) Importance of the vertical component of
534 groundwater flow: a hydrochemical approach in the valley of San Luis Potosí, Mexico. J
535 Hydrol 185:23-44

536 Carrillo-Rivera JJ, Cardona A, Edmunds WE (2002) Using extraction regime and knowledge
537 of hydrogeological conditions to control high-fluoride concentration in obtained groundwater:
538 San Luis Potosí basin, Mexico. J Hydrol 261:24-47

539 Carrillo-Rivera JJ, Varsányi I, Kovács L, Cardona A (2007) Tracing groundwater flow
540 systems with hydrochemistry in contrasting geological environments. Water Air Soil Pollut
541 184:77-103

542 Christiansen EH, Burt DM, Sheridan MF, Wilson RT (1983) The Petrogenesis of Topaz
543 Rhyolites from the Western United States. Contrib Mineral Petrol 83:16-30

544 Edmunds WM, Smedley PL (1996) Groundwater chemistry and health-an overview. In:
545 Appleton JD, Fuge R, McCall GJH (Eds.) Environ Geochem Health, Special Pub 113:91-105

546 Edmunds WM, Smedley PL (2000) Residence time indicators in groundwater: the East
547 Midlands Triassic sandstone aquifer. Appl Geochem 15(6):737-752

548 Edmunds WM, Ahmed KM, Whitehead PG (2015) A review of arsenic and its impacts in
549 groundwater of the Ganges-Brahmaputra-Meghna delta, Bangladesh. Environ Sci Process
550 Impacts 17(6):1032-1046

551 Fendorf S, Michael HA, Van Geen A (2010) Spatial and temporal variations of groundwater
552 arsenic in South and Southeast Asia. Science 328(5982):1123-1127

553 Gaciri SJ, Davies TC (1993) The occurrence and geochemistry of fluoride in some natural
554 waters of Kenya. J Hydrol 143:395-412

555 García-Pérez A, Irigoyen-Camacho ME, Borges-Yáñez A (2013) Fluorosis and Dental Caries
556 in Mexican Schoolchildren Residing in Areas with Different Water Fluoride Concentrations
557 and Receiving Fluoridated Salt. Caries Res 47:299-308

558 Grimaldo M, Borja-Aburto VH, Ramírez AL, Ponce M, Rosas M, Diaz-Barriga F (1995)
559 Endemic fluorosis in San Luis Potosí, México. Environ Res 68:25-30

560 Guidry MW, Mackenzie FT (2000) Apatite weathering and the Phanerozoic phosphorus
561 cycle. Geology 28(7):631-634

562 Guo H, Zhang Y, Xing L, Jia Y (2012) Spatial variation in arsenic and fluoride concentrations
563 of shallow groundwater from the town of Shahai in the Hetao basin, Inner Mongolia. Appl
564 Geochem 27:2187-2196

565 Guo H, Wen D, Liu Z, Jia Y, Guo Q (2014) A review of high arsenic groundwater in
566 Mainland and Taiwan, China: Distribution, characteristics and geochemical processes. Appl
567 Geochem 41:196-217

568 Guzmán EJ, De Cserna Z (1963) Tectonic history of México. Mem Am Assoc Pet Geol
569 2:115-120

570 INEGI (2013) Dirección General de Geografía. Continuo de Elevaciones Mexicano 3.0 (CEM
571 3.0). http://www.inegi.org.mx

572 Jia Y, Guo H, Jiang Y, Wu Y, Zhou Y (2014) Hydrogeochemical zonation and its implication
573 for arsenic mobilization in deep groundwaters near alluvial fans in the Hetao Basin, Inner
574 Mongolia. J Hydrol 518:410-420

575 Jia Y, Guo H, Xi B, Jiang Y, Zhang Z, Yuan R, Yi W, Xue X (2017) Sources of groundwater
576 salinity and potential impact on arsenic mobility in the western Hetao Basin, Inner Mongolia.
577 Sci Tot Environ 601-602:691-702

578 Labarthe-Hernández G, Tristán-González M, Aranda-Gómez JJ (1982) Revisión estratigráfica
579 del Cenozoico de la parte central del Estado de San Luis Potosí. Inst Geol Met UASLP
580 Folleto Técnico 85

581 Lambrakis N, Zagana E, Katsanou K (2013) Geochemical patterns and origin of alkaline
582 thermal waters in Central Greece (Platystomo and Smokovo areas). Environ Earth Sci
583 69:2475-2486

584 Lucas J (1988) Fluorine in the natural environment. J Fluorine Chem 41:1-8

585 McArthur JM, Sikdar PK, Hoque MA, Ghosal U (2012) Waste-water impacts on
586 groundwater: Cl/Br ratios and implications for arsenic pollution of groundwater in the Bengal
587 Basin and Red River Basin, Vietnam. Sci Tot Environ 437(11):390-402

588 Medellín-Milán P, Alfaro-De la Torre MC, De Lira-Santillán AG, Nieto-Ahumada B,
589 Sarabia-Meléndez I (1993) Fluoride in drinking water, its correlation with parameters of the
590 aquifer and effect on dental health in the City of San Luis Potosí, México. Proc. Water quality
591 Tech. Conf., Am. Water Works Assoc. 2:1011-1024

592 Navarro O, González J, Júnez-Ferreira HE, Bautista C-F, Cardona A (2017) Correlation of
593 Arsenic and Fluoride in the groundwater for human consumption in a semiarid region of
594 Mexico. Procedia Engineering 186:333-340

595 Négrel P, Millot R, Guerrot C, Petelet-Giraud E, Brenot A, Malcuit E (2012) Heterogeneities
596 and interconnections in groundwaters: Coupled B, Li and stable-isotope variations in a large
597 aquifer system (Eocene Sand aquifer, Southwestern France). Chem Geol 296-297:83-95

598 Nicolli HB, Garcia JW, Falcon CM, Smedley PL (2012) Mobilization of arsenic and other
599 trace elements of health concern in groundwater from the Sali River Basin, Tucuman
600 Province, Argentina. Environ Geochem Health 34:251-262

601 Nieto-Samaniego AF, Macías-Romo C, Alaniz-Álvarez S A (1996) Nuevas edades isotópicas
602 de la cubierta volcánica cenozoica de la parte meridional de la Mesa Central, México. Rev
603 Mexic Cienc Geol 13(1):117-122

604 Orozco-Esquivel MT, Nieto-Samaniego AF, Alaniz-Alvarez SA (2002) Origin of rhyolitic
605 lavas in the Mesa Central, Mexico, by crustal melting related to extension. J Volcanol
606 Geotherm Res 118:37-56

607 Parkhurst DL, Thorstenson DC, Plummer LN (1980) PHREEQC - A computer program for
608 geochemical calculations. USGS-Water Resources Investigations 90-92

609 Raju NJ (2017) Prevalence of fluorosis in the fluoride enriched groundwater in semi-arid parts
610 of eastern India: Geochemistry and health implications. Quaternary Intern 443:265-278

611 Rodríguez-Ríos R (1997) Caractérisation du magmatisme et des minéralisations associées du
612 dome de Pinos et des dômes de rhyolite à topaze du Champ Volcanique de San Luis Potosí
613 (Mexique). Dissertation, Université Henri Poincaré, Nancy

614 Sarabia MFI (1989) Contenido de fluoruros en el agua de consumo y sus efectos en el tejido
615 dental, San Luis Potosí, México. M.Sc. Thesis, Universidad Autónoma de San Luis Potosí

616 Stecher O (1998) Fluorine geochemistry in volcanic rock series: Examples from Iceland and
617 Jan Mayen. Geochim Cosmochim Acta 62(18):3117-3130

618 Stretta EJP, Del Arenal R (1960) Estudio para el abastecimiento del agua potable para la
619 ciudad de San Luis Potosí. Instituto de Ciencia Aplicada UNAM, México.

620 Tóth J (1998) Groundwater as a geological agent: An overview of the causes, processes, and
621 manifestations. Hydrogeol J 7:1-14

622 Tristán-González M (1986) Estratigrafía y tectónica del Graben de Villa de Reyes, en los
623 estados de San Luis Potosí y Guanajuato, México. Inst Geol UASLP, Folleto Técnico 10

624 Tristán-González M, Labarthe-Hernández G, Aguillón-Robles A, Torres-Hernández JR,
625 Aguirre-Díaz G (2006) Diques piroclásticos en fallas de extensión alimentadores de
626 ignimbritas en el occidente del Campo Volcánico del Río Santa María, S.L.P (resumen).
627 GEOS 26(1):163

628 Tristán-González M, Aguillón-Robles A, Barboza-Gudiño JR, Torres-Hernández, JR, Bellon,
629 H, López-Doncel, RA, Rodríguez-Ríos, R, Labarthe-Hernández, G (2009) Geocronología y
630 distribución espacial del Campo Volcánico de San Luis Potosí. Bol Soc Geol Mex 61(3):287-
631 303

632 Valenzuela-Vásquez L, Ramírez-Hernández J, Reyes-López J, Sol-Uribe A, Lázaro-Mancilla
633 O (2006) The origin of fluoride in groundwater supply to Hermosillo City, Sonora, México.
634 Environ Geol 51:17-27